Journal of Nepal Geological Society, 2025, Vol. 69, pp. 19-32
https://doi.org/10.3126/jngs.v69i1.88313

Geology, petrography and microstructures of upper part of the Kathmandu nappe along Balaju to Tadi Khola, northwest of Kathmandu, central Nepal

Rashmi Acharya and *Kabi Raj Poudyal

Central Department of Geology, Tribhuvan University, Kathmandu, Nepal
**Corresponding author's email: paudyalkabi1971@gmail.com*

ABSTRACT

This study analyzes the modal mineral composition and microstructural characteristics of rocks from the Balaju-Tadi Khola section to add some insightful information regarding the structural analysis of the region. This study investigates the geological distribution and metamorphic characteristics of the Kulikhani Formation (Bhimphedi Group) and the Tistung, Sopyang, and Chandragiri formations (Phulchauki Group) within the Kathmandu Complex. The northern region is composed of micaceous schist, laminated quartzite, and graphitic schist, while the central area is dominated by various types of gneiss, including augen gneiss, banded gneiss, and migmatite. The gneiss zone spans ~10-15 km in width and is associated with biotite-rich and tourmaline-bearing garnets. The study also identifies two main types of pegmatites: one rich in tourmaline and another in biotite. Petrographic analysis of 14 representative rock samples from the study area reveals a diverse range of metamorphic and sedimentary lithologies, highlighting a complex tectonometamorphic history. Graphitic schist and phyllite exhibit well-developed foliation with quartz, mica, and biotite, indicating moderate- to high-grade metamorphism. Quartzites and metasandstones show dynamic and static recrystallization features such as grain boundary migration and bulging, suggesting deformation at elevated temperatures. Gneissic samples display evidence of high-temperature metamorphism with foam-like textures and sutured grain boundaries. Garnet-bearing schists and calcsilicate rocks further confirm medium to high-grade metamorphic conditions. Limestones from the Sopyang Formation show recrystallization textures typical of low- to medium-grade metamorphism. The widespread presence of dynamic recrystallization across rock types suggests intense tectonic activity and prolonged deformation in the study region. The research shows the complex geological and metamorphic processes forming the Kathmandu Complex.

Keywords: Kathmandu Complex; Petrography; Dynamic recrystallization; Microstructure

Received: 14 May 2025 **Accepted:** 18 December 2025

INTRODUCTION

Within the Lesser Himalaya of Central Nepal lies the Kathmandu Complex, which forms a significant tectonostratigraphic unit composed predominantly of highly deformed and metamorphosed sedimentary and low-grade metamorphic rocks. The Lesser Himalaya represents the fold-and-thrust belt of the Himalayan orogen. Hagen (1969) introduced the concept of nappes in this region. Hashimoto et al. (1973) divided the Kathmandu area into several lithostratigraphic zones, such as the Gosaikund Gneiss Zone, Main Central Thrust (MCT) Zone, Nawakot Metasediment Zone, and others. They also classified the Midland Metasediment Group into four lithological successions: calcareous, siliceous, arenaceous, and argillaceous. Later, Stöcklin (1980), building on Hagen's ideas, interpreted the Kathmandu Complex as the "Kathmandu Nappe", derived from the Central Crystalline Zone, and considered the Mahabharat Thrust (MT) as a continuation of the MCT. He described a regional metamorphic sequence with decreasing grade from garnet-rich schists at the base to fossil-bearing sediments at the top. A later phase of high-temperature metamorphism is suggested by the presence of gneisses. The Kathmandu Complex in the Nuwakot area exposes a variety of lithologies, including schist, quartzite, schist, metasandstone, limestone, which are suitable for detailed structural and lithological investigation.

The petrographic and microstructural study is a crucial tool to accurately identify and classify the various rock types, determine the metamorphic grade of the region, and analyze the deformation history, tectonic setting, and evidence of both static and dynamic recrystallization processes. This research focuses on the petrography and microstructural analysis of the Balaju-Tadi road region in northern Kathmandu Valley to better understand local tectonic evolution. At the end point, the study will address the issues related to the petrographic identification and characterization of minerals and their structures to relate them to the metamorphic history and the tectonic evolution of the area.

STUDY AREA

The Nuwakot and Kathmandu districts, located in Bagmati Province of central Nepal, cover an area of approximately 300 km². Geographically, the region lies between latitudes 27°45’00” to 27°52’00” N and longitudes 85°07’30” to 85°17’30” E. The present study lies in the northwest part of Kathmandu district (Fig. 1). The district has a varied topography, with elevations between 600 m and 2700 m above mean sea level. The study area can be easily reached from Kathmandu via the Pasang Lhamu Highway, taking about four to five hours by local bus. Geographically, the area lies in a hilly region with steep slopes, uneven landforms, and rocky ground. Geologically, it lies within the Lesser Himalayan zone and mainly includes rocks from the Bhimphedi Group and the Phulchauki Group of the Kathmandu Complex.

METHODOLOGY

After reviewing previous studies and relevant literature, fieldwork was done to prepare a geological map of the Balaju to Tadi Khola section at a 1:25,000 scale. During fieldwork, orientation and systematic rock samples were collected from each rock type in every lithological unit. Thin sections were prepared from selected rock samples by cutting them as perpendicular as possible to bedding and foliation, and parallel to linear features at the Central Department of Geology. The main focus was to identify minerals in paragenesis and observe microstructures like static and dynamic recrystallization using a petrological microscope. Volumetric concentrations were estimated through visual observation. The analysis focused on the mineral's texture, compositional zoning, grain size, and drawing the metamorphic structures present in the rocks. Under the microscope, features like different sets of cleavage and foliation, their orientations, microfolds, and pre-tectonic garnet were examined. Different types of recrystallization such as grain boundary area reduction, bulging, window structures, and pinning-were studied to understand the rock deformation patterns. Special attention was given to quartz and garnet microstructures to interpret the deformation and metamorphic conditions. Finally, the microstructures and index minerals were used to identify geological structures in the area and define the metamorphic zonation and deformation history.

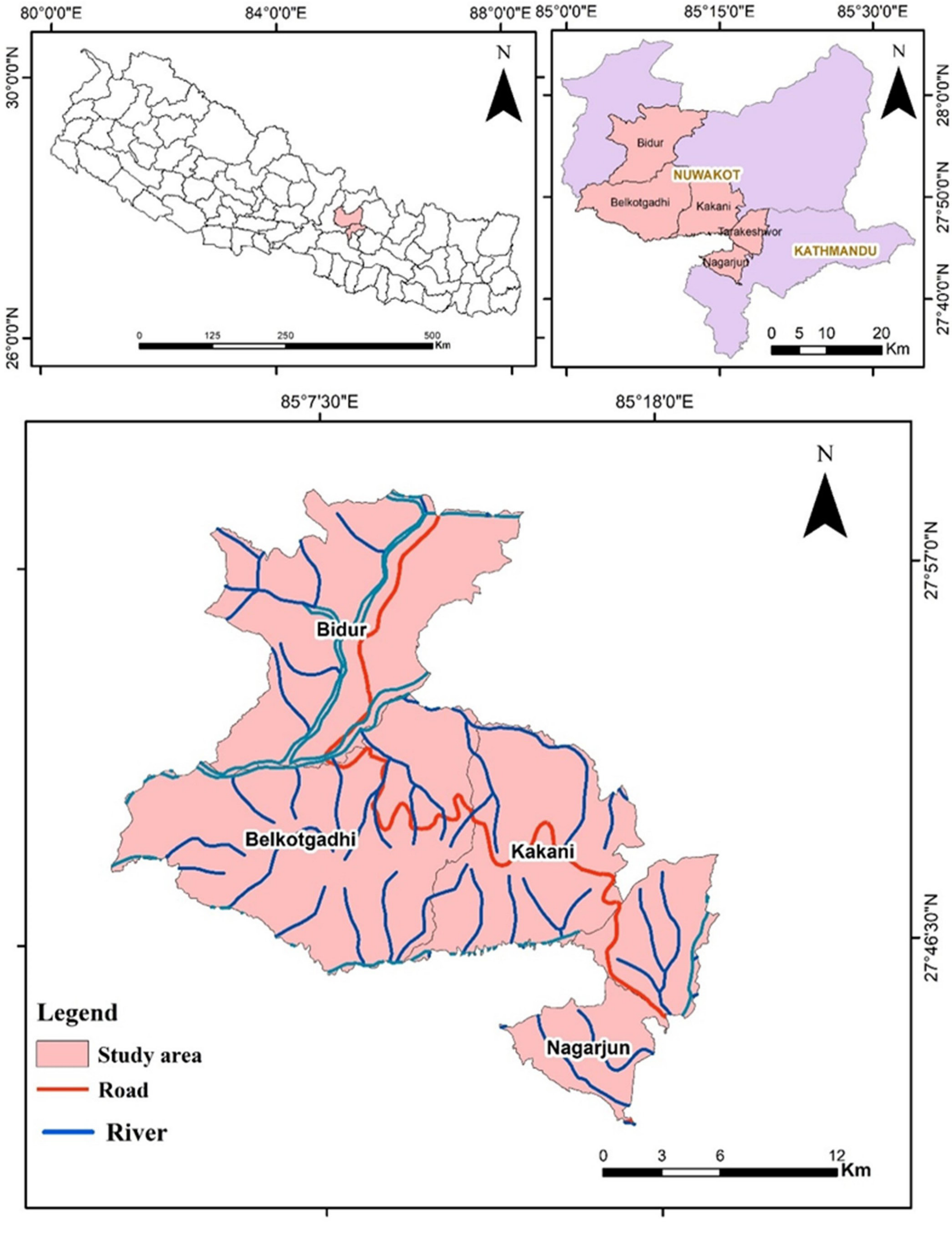

Fig. 1: Political map of Nepal and location map of study area.

PREVIOUS WORKS

Early geological investigations in Central Nepal began with Medlicott (1875), who discovered the fossil-bearing Chandragiri-Phulchauki beds and reported high-grade gneisses north of Kathmandu. Auden (1934) observed the overlying relationship of high- and low-grade metamorphic rocks in the Mahabharat Range and linked the Shivapuri Injection Gneiss with the Darjeeling Gneiss. Bordet et al. (1960) verified the Silurian age of basal Phulchauki rocks using trilobite fossils and extended their work into central-west Nepal (Bordet et al. 1964, 1972). Hagen (1969) classified two distinct rock series- the older Kathmandu Series and the younger Nawakot Series- suggesting the Kathmandu unit was emplaced tectonically over the Nawakot sequence. He related them to thrust structures similar to the Alps and identified a tectonic connection via the Gosainkunda Gneiss. Burnel (1975) supported the klippe model for the Kathmandu rocks but disputed Hagen's multiple nappe theory. Nagdir et al. (1968–1973) described the Kathmandu-Nuwakot boundary as intraformational thrusting and attributed metamorphism in Kathmandu rocks to granitic intrusions. Ohta and Akiba (1973) refuted the nappe model and proposed a continuous metamorphic sequence separated by a steep fault near Sheopuri Lekh, based on lithological and structural correlations. Hashimoto et al. (1973) divided the Kathmandu region into several lithostratigraphic zones and categorized the Midland Metasediments into four types: calcareous, siliceous, arenaceous, and argillaceous successions. Stöcklin and Bhattarai (1977) conducted mineral exploration in central Nepal and later, Stöcklin (1980) interpreted the Kathmandu Complex as a large thrust sheet or nappe from the Central Crystalline Zone. Rai et al. (1998), Upreti and Le Fort (1999), and Upreti (1999) placed the Main Central Thrust (MCT) north of the Kathmandu Valley and proposed that it emplaced the Gosainkund Crystalline Nappe over the Kathmandu Crystalline Nappe. They considered the MCT a distinct structure rather than a simple southern extension. Upreti (1999) classified Lesser Himalayan crystalline nappes into two groups based on metamorphic grade: (1) high-grade nappes similar to Higher Himalayan rocks, and (2) lower-grade nappes, such as the Bhimphedi Group, which includes the Kathmandu Nappe. Upreti and Le Fort (1999) further suggested that the Mahabharat Thrust (MT), located south of the MCT, succeeded the MCT in accommodating tectonic displacement. The MT uplifted the Bhimphedi Group rocks over the Lesser Himalaya. Passchier and Trouw (2005) emphasized the significance of microstructural analysis in understanding deformational and metamorphic processes, as rock fabrics preserve the history of deformation events. Thapaliya and Paudel (2011) investigated the Kathmandu Nappe and Lesser Himalayan units along the Pasang Lhamu Highway. They identified formations such as the Kunchha Formation, Benighat Slate, and Robang Formation within the Nawakot Complex, and the Kalitar, Tistung, Sopyang, and Chandragiri formations in the Kathmandu Nappe. Petrographic evidence indicated inverted metamorphism with biotite zones in the Kunchha Formation and garnet zones in the Benighat and Robang formations. Sapkota (2011) studied garnet-bearing mylonites in the Kathmandu Thrust sheet, highlighting a complex tectonometamorphic history near the MCT, further complicated by folding (e.g., the Gorkha-Kathmandu fold couplet).

Paudyal and Paudel (2013) revised the stratigraphy and structure of the Nawakot Group west of the Mugling-Damauli area. They identified the Kahun Klippe as part of a larger crystalline thrust sheet that includes the Kathmandu and Jajarkot Klippes. They equated the Dubung Thrust with the Mahabharat Thrust and proposed that the Bhimphedi Group was emplaced over the Nawakot Complex by the MCT. Paudyal (2014) identified five deformation phases in the Mugling-Damauli region-two pre-Himalayan and three Himalayan. These included isoclinal folding, south-vergent folds, crenulation cleavage, and brittle faulting. Inverted metamorphism was also recognized at the root zones of both the MCT and the Dubung Thrust (equivalent to the MT). Acharya et al. (2015) studied the western Kathmandu Nappe (Galchhi-Malekhu) and concluded that its structural and metamorphic features represent a re-entrant of the MCT within the thrust belt. Subedi and Acharya (2016) investigated the Bhainse-Manahari area, identifying the Nawakot Complex and Kathmandu Complex, separated by the Mahabharat Thrust. The Kathmandu Complex is composed of medium-grade metamorphic rocks, while the Nawakot Complex contains low-grade rocks. The study identified strong deformation along the MT, with strain and shear indicators suggesting it functions as a stretching fault.

GEOLOGICAL SETTING OF THE AREA

The geological map (Fig. 2) shows the rock distribution of Kulikhani Formation of Bhimphedi Group and Tistung Formation, Sopyang Formation and Chandragiri Limestone of Phulchauki Group of Kathmandu Complex. In the northern part of the region, the Kulikhani Formation is made up of micaceous schist, laminated quartzite, and graphitic schist (Figs. 3a, b, and c). The central area is mainly covered by the gneiss zone, which is dominant in the study area. This zone includes different types of gneiss, such as augen gneiss, banded gneiss, migmatite, calcsilicate gneiss, hornblende gneiss. Much of the Bhimphedi Group within the Kathmandu Complex has undergone metamorphism, i.e. metamorphosed into gneiss (with granite and pegmatite intrusions) and migmatite. The gneiss zone covers about 10 to 15 km in width and is commonly associated with biotite-rich and tourmaline-bearing garnets. The augen gneiss is elongated and aligns parallel to the foliation of the surrounding rock and the size of the augen varies from 2 mm to 10 mm. Concordant pegmatite vein along with augen gneiss was observed at 250 south of Dharna Khola (kholsi) (Fig. 3d) and the migmatite gneiss is observed at 200 m south of the Jurethum area along the Passang Lamhu Highway. Migmatites in the study area often appear as tightly folded veins, known as ptygmatic folds. The migmatite gneiss here is mainly composed of quartz, feldspar, hornblende, and biotite (Fig. 3e). This zone contains alternating layers of calcareous and non-calcareous gneiss interspersed with bands of white marble. Light to dark grey, thin- to medium-bedded calc-silicate gneiss with a bone-like structure is observed in

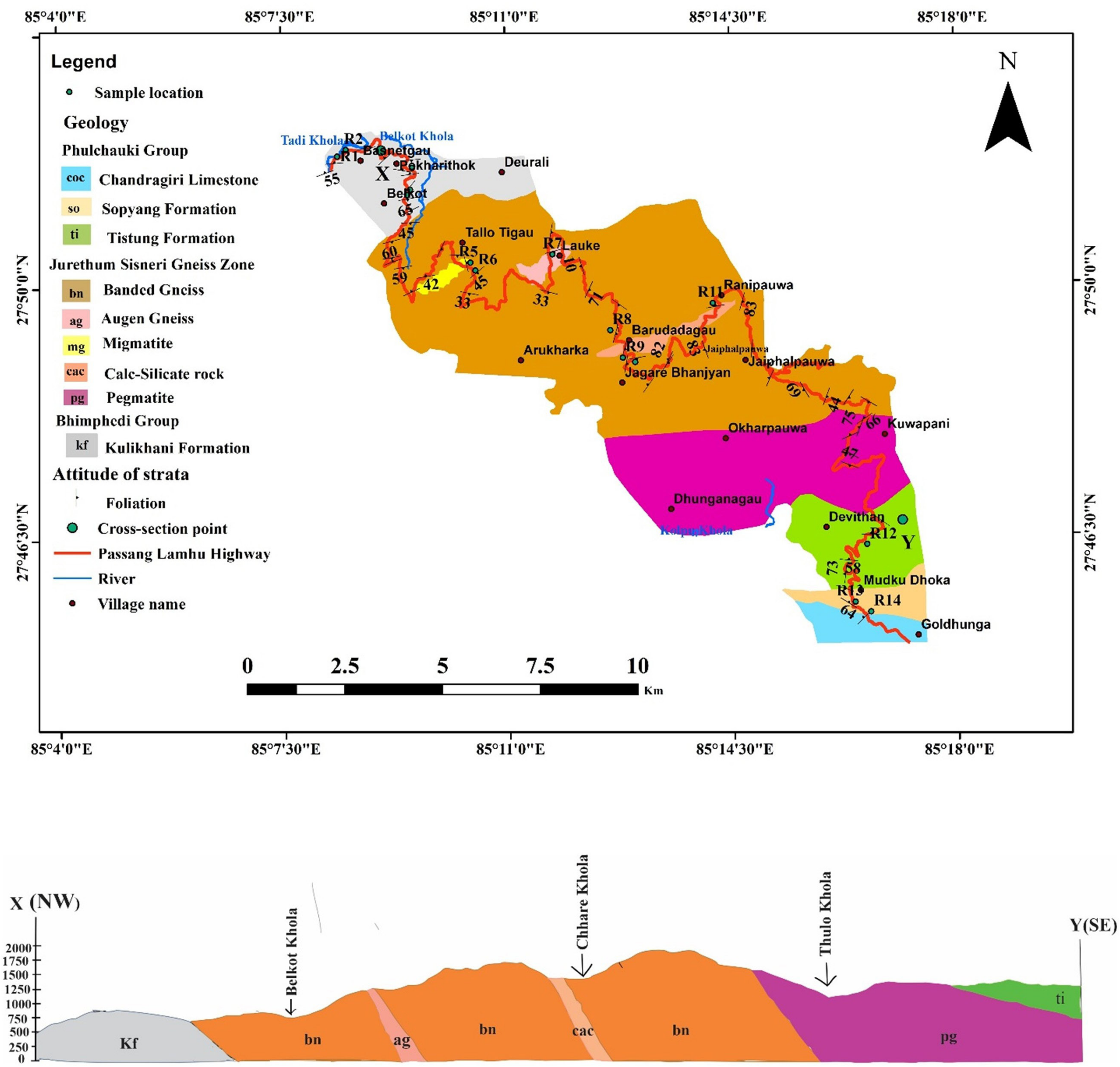

Fig.2: Geological map of Balaju-Tadikhola section with petrography sample location and showing the cross section along Basnetgau (X)-Devithan (Y).

the study area (Fig. 3f). Pegmatites are well-exposed between the Khanigau and Nanedadagau along the Passang Lamhu Highway and the upper part of the Tistung Formation. In the study area, there are two main kinds of pegmatite present: one abundant in tourmaline and another abundant in biotite. In the biotite-rich pegmatite, biotite is the primary dark mineral, with occasional or no presence of tourmaline and muscovite (Fig. 4a). The dominant lithology in the study area consists of phyllite and metasandstone, with minor amounts of quartzite. The lower section of Tistung Formation is made up of fine- to medium-grained greenish to grey phyllite and metasandstone (Fig. 4b). The Sopyang Formation is primarily composed of slate, with minor amounts of limestone and sandstone. It represents a transitional boundary between the upper Chandragiri Limestone and the lower Tistung Formation. Several small-scale folds are present within this unit. About 250 meters north of Osho Tapoban, the lower section includes gray slate featuring an S-type small-scale fold, along with some fine- to medium-grained gray sandstone (Fig. 4c). The Chandragiri Limestone is prominently exposed between the Bainkhu and Balaju bypass areas along the Pasang Lhamu Highway, situated on the northern slope of Nagarjun Hill. This hill is predominantly composed of Chandragiri Limestone, which constitutes a significant lithostratigraphic unit in the region. The formation primarily consists of fine-grained, dirty white to light yellow limestone, with intercalations of quartzite. In the study area, the lower stratigraphic portion of this unit is characterized by fine-grained, argillaceous, gray, wavy-bedded limestone, with occasional lenses and layers of quartzite (Fig. 4d).

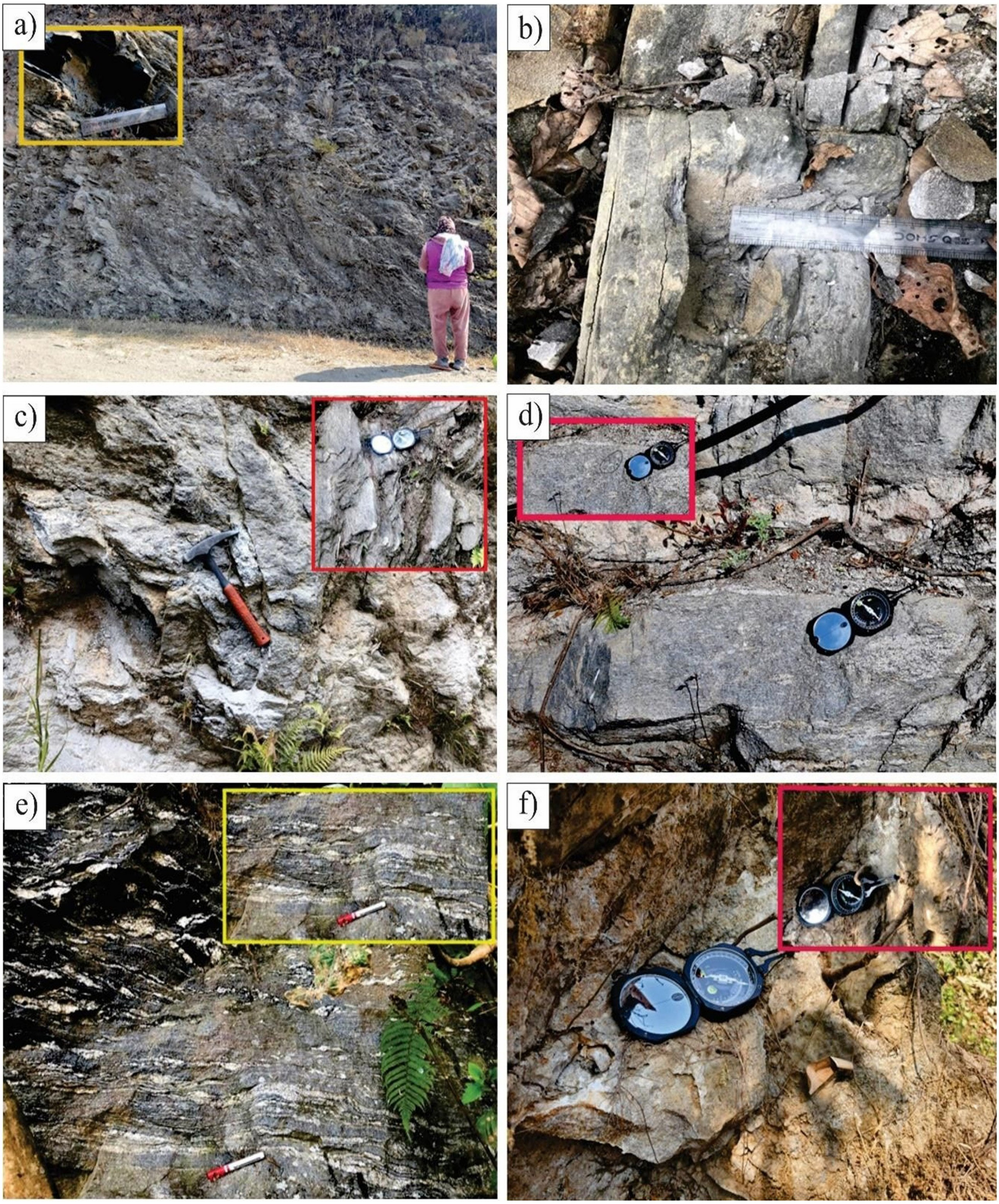

Fig. 3: Outcrop photographs: a) Dark black Graphitic schist of Kulikhani Formation, b) amphibolite of Kulikhani Formation, c) micaceous schist of Kulikhani Formation, d) elliptical shaped augen gneiss observed in Beteni forest, e) ptygmatic fold of migmatite gneiss observed near Sisneri, f) calc-silicate gneiss observed in Barudadagaun area.

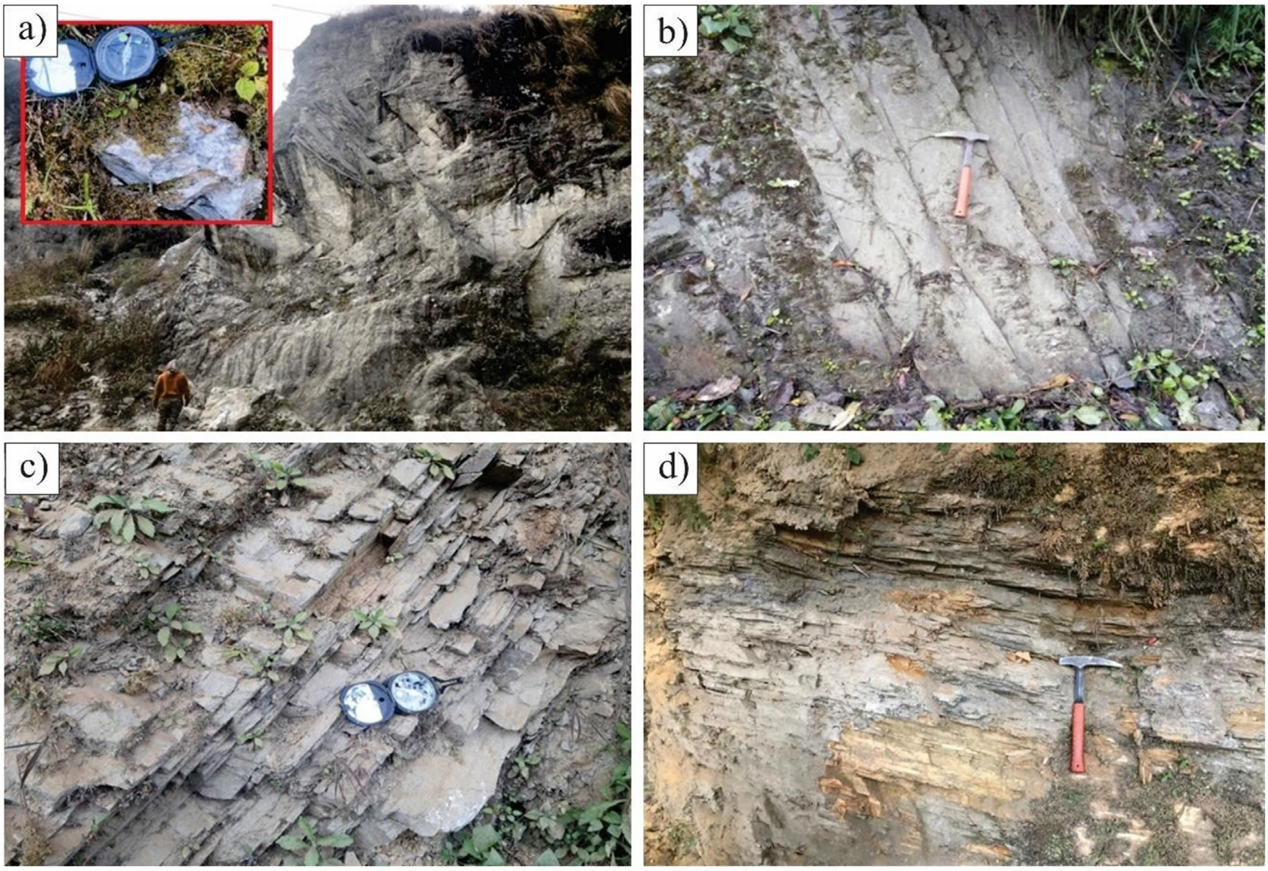

Fig. 4: Outcrop photographs of Phulchauki Group: a) Weathered exposure of pegmatite and left to the top showing the fresh pegmatite observed in Padali area, b) dark grey metasandstone of Tistung Formation observed in Tinpiple, c) marl Limestone of Sopyang Formation observed in Mudku Dhoka area, and d) weathered grey limestone of Chandragiri Limestone observed in Nakhandol area.

Petrography

Fourteen thin sections representing each stratigraphic unit were studied to analyze the texture, structures, and mineral paragenesis under a polarizing microscope (Table 1).

Table 1: Sample details used for the microscopic analysis

S.N	Sample Symbol	GPS location	Attitude	Formation
1	R1	27°51'38.02"N, 85° 9'19.00"E	280/65/190	Kulikhani Formation
2	R2	27°51'35.83"N, 85° 9'25.92"E	262/50/172	
3	R3	27°51'38.01"N, 85° 8'6.05"E	250/55/163	
4	R4	27°51'22.05"N, 85° 9'17.83"E	60/45/135	
5	R5	27°50'16.79"N, 85°10'15.59"E	345/78/255	Sisneri-Jurethum Gneiss
6	R6	27°50'16.17"N, 85°10'16.52"E	30/31/118	
7	R8	27°49'22.77"N, 85°12'36.31"E	10/20/100	
8	R9	27°49'3.54"N, 85°12'40.91"E	15/13/105	
9	R10	27°48'51.13"N, 85°12'42.89"E	10/8/100	
10	R11	27°49'43.94"N, 85°14'10.82"E	260/83/170	
11	R12	27°47'29.80"N, 85°16'6.33"E	110/47/20	Tistung Formation
12	R7	27°50'4.35"N, 85°11'35.11"E	105/33/195	Augen Gneiss
13	R13	27°45'33.56"N, 85°16'12.67"E	302/ 64/212	Sopyang Formation
14	R14	27°45'11.12"N, 85°16'51.05"E	225/30/315	Chandragiri Limestone

Sample R1

Sample R1 was collected approximately 250 meters south of Tadipul Chhahare and is identified in hand sample as a black graphitic schist. This rock unit is part of the middle section of the Kulikhani Formation**.** Under thin section analysis, the sample is predominantly composed of graphitic material (~50%), along with quartz (~25%), and a mixture of mica (~25%). The presence of biotite, a metamorphic index mineral, indicates metamorphic conditions. The rock shows alternating light (quartz-rich) and dark to brown (graphite-rich) bands, with a preferred alignment of micaceous minerals, defining a well-developed foliation (Fig. 5a).

Sample R2

Sample R2, collected about 350 meters south of the Pokharithok area, is identified as quartzite in hand sample. This sample represents the middle part of the Kulikhani Formation. In thin section, the rock is mainly composed of quartz (~90%) and mica (~10%). Quartz grains are anhedral to subhedral, ranging from 0.15 mm to 0.25 mm in size, and show an inequigranular texture with interlobate to amoeboid grain boundaries. Photomicrograph 2 shows features of both dynamic and static recrystallization. Grain Boundary Migration (GBM) and Grain Boundary Area Reduction (GBAR) are observed, with the foam-like structures and triple junctions suggesting static recrystallization (GBAR). Bulging textures indicate dynamic recrystallization, likely involving the development of sub-grain boundaries and new grains. similarly, mica pushing into adjacent quartz grains, forming window structures (highlighted by a black circle), also points to dynamic recrystallization processes (Fig. 5b).

Sample R3

Sample R3, collected about 50 meters south of Tadipul Chhahare, is identified as a green laminated phyllite in hand sample. It belongs to the lower section of the Kulikhani Formation. Thin section analysis shows the rock is composed of approximately 60% quartz, 30% mica and sericite. The alignment of these minerals defines the foliation planes. Quartz grains are anhedral to subhedral, ranging in size from 0.05 mm to 0.15 mm, and display inequigranular textures with amoeboid and irregular grain boundaries. The recrystallized mineral assemblage includes sericite, quartz, chlorite, and biotite. Evidence of dynamic recrystallization is seen through Grain Boundary Migration (GBM), with relict quartz grains retaining some original features, suggesting high-temperature deformation (Fig. 5c).

Sample R4

Sample R4, collected approximately 250 meters north of Apchaur along the Passang Lamhu Highway, is identified as a grey garnet schist in hand sample. It belongs to the upper section of the Kulekhani Formation. In thin section, the rock is mainly composed of quartz (~60%) and mica (~30%). Quartz grains are anhedral to subhedral, ranging in size from 0.05 to 0.15 mm, and display inequigranular to interlobate textures. Garnet porphyroblasts are also present (Fig. 5d) and are interpreted as pre-tectonic, based on the presence of inclusions with random orientation (top-to-the-south shear sense) within the garnet.

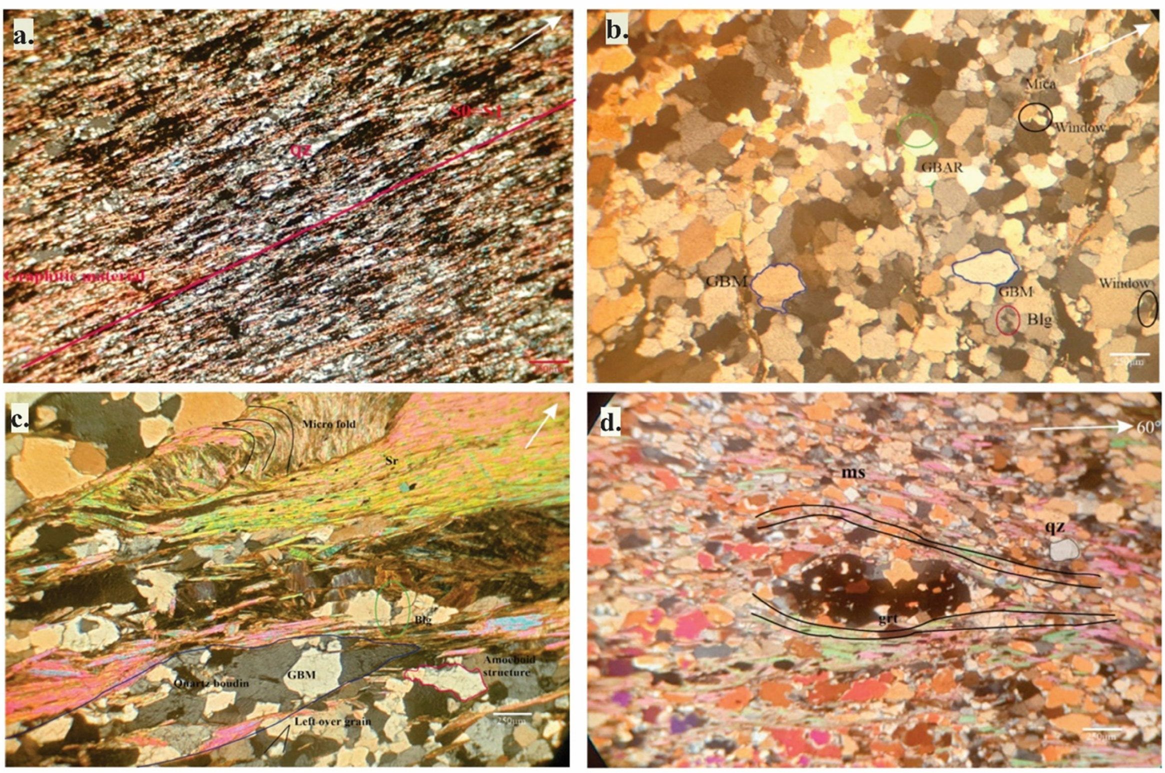

Fig. 5: Photomicrograph of samples under cross-polarizing light: a) One set of distinct foliation planes (s1) in graphitic schist of Kulikhani Formation observed under 10x magnification, b) quartzite showing both static and dynamic recrystallization of Kulikhani Formation under 10x magnification, c) phyllite of Kulikhani Formation showing dynamic recrystallization and microfolds (N-S) trending observed in 10x magnification, and d) schist of Kulikhani Formation showing pre-tectonic garnet observed in 10x magnification.

Sample R5

Sample R5, collected about 50 meters south of Tadipul Chhahare, is identified as a green laminated phyllite in hand sample. It belongs to the lower section of the Kulikhani Formation. Thin section analysis shows the rock is composed of approximately 60% quartz, 30% mica and sericite. The alignment of these minerals defines the foliation planes. Quartz grains are anhedral to subhedral, ranging in size from 0.05 mm to 0.15 mm, and display inequigranular textures with amoeboid and irregular grain boundaries. The recrystallized mineral assemblage includes sericite, quartz, chlorite, and biotite. Evidence of dynamic recrystallization is seen through Grain Boundary Migration (GBM), with relict quartz grains retaining some original features, suggesting high-temperature deformation (Fig. 6a).

Sample R6

Sample R6, collected approximately 500 meters south of Tallo Tigau along the Passang Lamhu Highway, is described in hand sample as a grey, fine-grained ortho-gneiss with a quartz vein. The sample represents the middle section of the Gneiss Zone. Under thin section analysis, it is composed of approximately 35% quartz, 50% alkali and K-feldspar, and 15% mica. Quartz grains are polygonal and display foam-like textures, with amoeboid grain boundaries, ranging in size from 0.05 mm to 0.25 mm (see Photomicrograph 10, black circle). K-feldspar grains are notably larger (1 mm to 1.5 mm) and exhibit features such as bulging recrystallization and undulose extinction, indicating dynamic recrystallization. Relict grains also support this interpretation. Photomicrograph 10 shows a deformation band in the left-central area and a mica fish in the right-central area, suggesting a top-to-the-south shear sense. The presence of irregular, amoeboid grain boundaries further supports grain boundary migration, indicating high-temperature dynamic recrystallization likely formed at temperatures between 500°C and 700°C, associated with a rapid recrystallization rate (Fig. 6b)

Sample R7

Sample R7 was collected approximately 550 meters south of the Pakhure along the Passang Lamhu Highway. In the thin section, the rock is composed of quartz (~35%), K-feldspar (~45%), and biotite (~10%) and mica (~5%). Quartz is euhedral to anhedral and grain sizes range from 0.05 mm to 0.25 mm, while K-feldspar is elongated and extends upto 2 mm. The irregular boundary of grains indicates the GBM. The pinning structure is associated with quartz and mica is observed. The Bulging (BLG) can also be seen within the quartz, which defines dynamic recrystallization (Fig. 6c).

Sample R8

Sample R8, collected about 500 meters south of Jurethum along the Passang Lamhu Highway, is identified as a coarse-grained, deformed granitic banded gneiss. It represents the middle part of the Gneiss Zone. In thin section, the rock is composed of approximately (~)30% quartz, (~20%) plagioclase and biotite, and (~10%) garnet. Quartz grains are amoeboid, inequigranular, and range from anhedral to subhedral, with sizes between 0.05 mm and 0.25 mm. Plagioclase grains are larger, extending up to 1.5 mm. Irregular grain boundaries indicate Grain Boundary Migration (GBM), a feature of high-temperature metamorphism. This supports the origin of granitic gneiss from high-grade metamorphism of granite. Biotite, showing high relief, stands out from the surrounding matrix. Undulate extinction in quartz, as shown in Photomicrograph 14, and bulging recrystallization, where small grains separate from larger ones through sub-grain formation (Fig. 6).

Sample R9

Sample R9 was collected approximately 100 meters south of Barundadagau along the Passang Lamhu Highway. It is a grey, fine-grained banded gneiss and is from the middle section of the Gneiss Zone. In the thin section, the rock is dominantly composed of quartz (~45%) k-feldspar (~45%), and mica (~10%). Sample G79 was collected approximately 100 meters south of Barundadagau along the Passang Lamhu Highway. It is a grey, fine-grained banded gneiss and is from the middle section of the Gneiss Zone. The quartz in the thin section grain sizes range from 0.15 to 0.55mm, while the K-feldspar has grain sizes upto 0.81 mm. These grains are subhedral to euhedral in shape and exhibit an inequigranular texture with sutured grain boundaries. The black circle indicates the sutured structure, which shows irregular and convoluted grain boundaries between adjacent minerals, indicating dynamic recrystallization. Similarly, mica shows pinning structures, which develop during dynamic recrystallization and may appear quartz convoluted near the mica, as indicated by the blue and black rectangles in Fig. 14. Window structure is also observed, further demonstrating the dynamic recrystallization process (Fig. 7a).

Sample R10

Sample R10, collected approximately 100 meters south of Sisneri along the Passang Lamhu Highway, is identified as a banded, deformed granitic gneiss and belongs to the middle part of the Gneiss Zone. In thin section, the rock consists of approximately 30% quartz, 45% plagioclase, and 15% biotite. Quartz grains are amoeboid, inequigranular, and range from anhedral to subhedral, with sizes around 0.25 mm. Plagioclase grains are elongated, extending up to 1.7 mm. The quartz displays irregular, convoluted grain boundaries, characteristic of dynamic recrystallization through grain boundary migration (GBM). Bulging (BLG) textures within quartz grains indicate recrystallization at relatively lower temperatures. A leftover grain, marked by a black arrow in Photomicrograph 15, is surrounded by larger recrystallized grains. This relict grain preserves features of the original crystal and reflects deformation at higher temperatures compared to the nearby bulging quartz (Fig. 7b).

Sample R11

Sample R11 was collected about 100 meters north of Ranipauwa along the Passang Lamhu Highway. It is a coarse-grained, dark grey cal-silicate rock observed in hand sample and is part of the upper Gneiss Zone. In thin section, the rock is mainly composed of quartz (~40%), calcite (~40%), K-feldspar (~10%), and minor amounts of biotite and garnet (~10%). Quartz grains are amoeboid, inequigranular, and range from anhedral to subhedral, with sizes between 0.05 mm and 0.25 mm. K-feldspar grains are anhedral, reaching up to 1 mm. Only a small amount of mica is observed. Figure 7c shows features of dynamic recrystallization, where bulging quartz grains appear to separate from host grains and form new, smaller grains along grain boundaries. Calcite grains, as shown in Fig. 16, show twinning and sutured grain boundaries, which are characteristic of grain boundary migration (GBM), another indicator of dynamic recrystallization. Some calcite grains display distinct lamellae, supporting deformation under metamorphic conditions.

Sample R12

Sample R12, collected approximately 200 meters north of Jalukeni along the Passang Lamhu Highway, is a grey metasandstone with a thin- to medium-bedded, coarse-grained texture. This sample represents the upper part of the southern section of the study area. In thin section, the rock is primarily composed of quartz (~30%), K-feldspar (~20%), biotite and muscovite (~20%), opaque minerals (~15%), and chlorite (~15%). Quartz grains are colorless, range from subhedral to anhedral, and are generally fine-grained, with an average size of ~0.15 mm. These grains exhibit irregular, folded boundaries, a sign of grain boundary migration (GBM) and dynamic recrystallization. Figure 7d shows folded or irregularly shaped quartz grains with sutured contacts, supporting the evidence of GBM. Brown biotite and green chlorite are also present and clearly visible in the photomicrograph. The dominance of fine quartz grains and their irregular boundaries suggests rapid recrystallization during deformation under metamorphic conditions.

Sample R13

Sample R13, collected approximately 250 meters north of Mudku Dhoka along the Passang Lamhu Highway, is identified as a grey marl limestone and belongs to the lower section of the Sopyang Formation. In thin section, the rock

Fig. 6: Photomicrograph of samples under cross polarizing light; a) Granite showing sutured contact and mica fish observed in 10x magnification (27°50'16.79"N, 85°10'15.59"E), b) showing both dynamic and static recrystallization observed in 10x magnification (27°50'16.17"N, 85°10'16.52"E), c) showing dynamic recrystallization and triple junction observed in 10x magnification (27°50'4.35"N, 85°11'35.11"E), and d) granitic gneiss showing big, wavy extinction observed in 10x magnification (27°49'22.77"N, 85°12'36.31"E).

is primarily composed of calcite and dolomite (~90%), with quartz (~10%). Quartz grains are irregular in shape and reach up to 0.10 mm in size, while calcite grains are elongated, with sizes up to 0.60 mm. Some calcite grains form 120° triple junctions, indicating grain boundary area reduction during recrystallization. Both calcite and dolomite display a single set of polysynthetic twinning, and twin lamellae within the calcite grains are clearly visible in Fig. 8a.

Sample R14

Sample R14 was collected approximately 350 m north of Mudku Dhoka along the Passang Lamhu Highway. In thin section, the rock is mainly composed of calcite and dolomite (~90%), with about 10% quartz. Quartz grains are irregular in shape and reach sizes up to 0.10 mm, while calcite grains are larger, extending up to 0.70 mm. Both calcite and dolomite display a single set of twinning, which is clearly visible in Fig. 8b.

DISCUSSION

The lithological and structural features observed in the study area reflect a complex geological history involving intense metamorphism and deformation, characteristic of the Kathmandu Complex. The geological map delineates the distribution of various formations including the Kulikhani Formation of the Bhimphedi Group, and the Tistung, Sopyang, and Chandragiri Limestone formations of the Phulchauki Group.

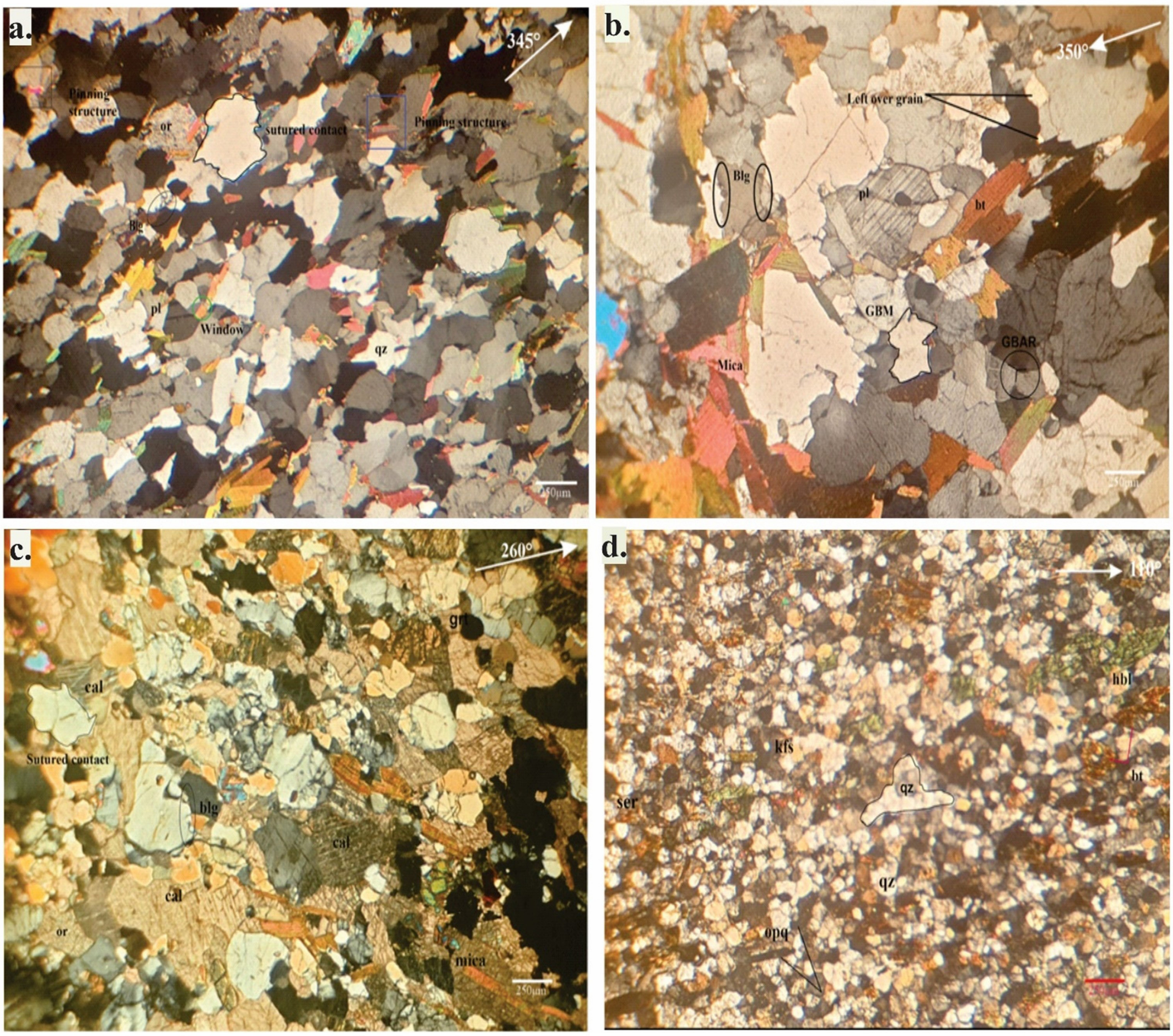

Fig.7: Photomicrograph of samples under cross polarizing light: a) Showing sutured, pinning window strctures observed near Sisneri area under cross polarizing light (27°49'3.54"N, 85°12'40.91"E), b) granitic gneiss showing both dynamic and static recrystallization under cross polarizing light (27°48'51.13"N, 85°12'42.89"E), c) calc-silicate gneiss showing Blg, calcite observed near Ranipauwa park under cross polarizing light (27°49'43.94"N, 85°14'10.82"E), and d) metasandstone from Tistung Formation observed near Jalukelp showing the irregular boundary of quartz crystals Under cross polarizing light (27°47'29.80"N, 85°16'6.33"E).

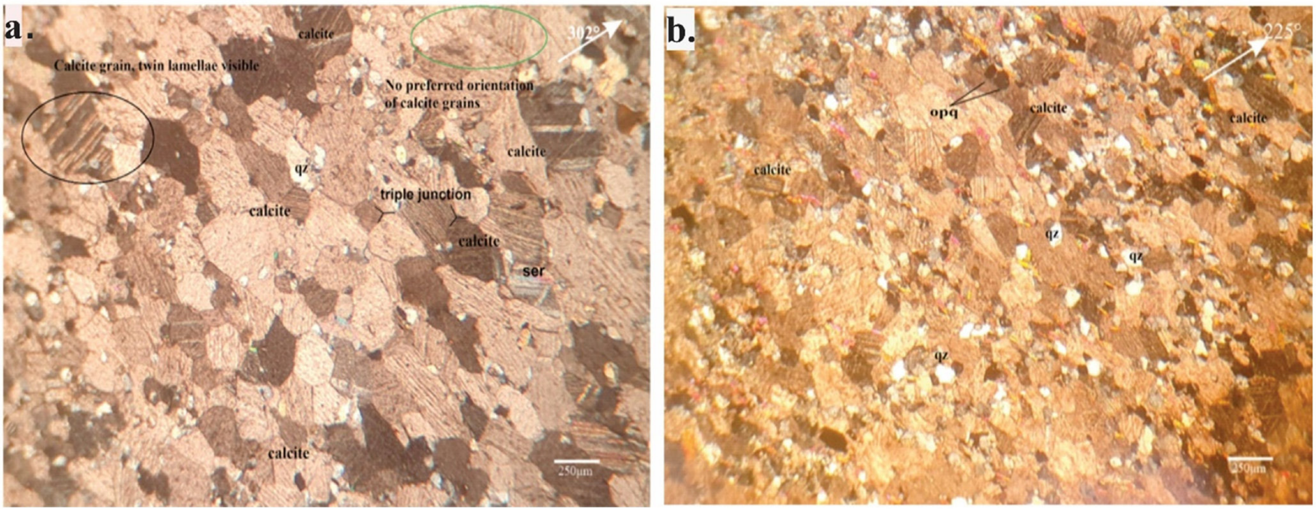

Fig. 8: Photomicrograph of sample under polarizing light: a) Marl limestone showing the calcite grain, twin lamella and no preferred orientation of calcite grains observed in Mudku Dhoka area (27°45'33.56"N, 85°16'12.67"E) and b) grey Limestone of Chandragiri Limestone showing (~80%) calcite and (~15%) quartz) observed in Nakhandol area under cross polarizing light (27°45'33.56"N, 85°16'12.67"E).

In the northern part of the study area, the Kulikhani Formation is dominated by medium- to high-grade metamorphic rocks such as micaceous schist, laminated quartzite, and graphitic schist (Fig. 3a). These lithologies suggest significant tectono-thermal events that transformed the original sedimentary protoliths. The central portion of the area is occupied by a prominent gneissic zone, approximately 10-15 km wide, representing the metamorphic core of the Bhimphedi Group. This zone includes a variety of gneiss types: augen gneiss, banded gneiss, calc-silicate gneiss, hornblende gneiss, and migmatite, indicating variable protolith composition and metamorphic conditions. Augen gneiss, with its elongate feldspar grains aligned parallel to foliation, shows grain sizes ranging from 2 mm to 10 mm. Concordant pegmatite intrusions associated with this unit, such as those found 250 m south of Dharna Khola, further support high-grade metamorphism and partial melting processes. Migmatitic gneiss, observed notably 200 m south of the Jurethum area, displays classic ptygmatic folding, reflecting intense ductile deformation. The migmatite consists mainly of quartz, feldspar, hornblende, and biotite, confirming partial melting of the host rock under anatectic conditions. Alternating layers of calcareous and non-calcareous gneiss, along with interbands of white marble, highlight the compositional diversity and fluid activity during metamorphism. Calc-silicate gneiss with distinctive bone-like textures (Fig. 3c) suggests metasomatic alteration processes, possibly in a contact metamorphic setting. Pegmatites are widespread, particularly between Khanigau and Nanedadagau and within the upper parts of the Tistung Formation. These pegmatites are classified into two types: tourmaline-rich and biotite-rich. The biotite-rich variant, characterized by the dominance of biotite and minimal muscovite and tourmaline (Fig. 4), further indicates crystallization from volatile-rich residual melts. The southern region exhibits low- to medium-grade metamorphic rocks such as phyllite and metasandstone, with minor quartzite components. These lithologies, especially the greenish to grey phyllite and metasandstone, mark the transition between high-grade gneissic units and less metamorphosed sedimentary units. The Sopyang Formation represents a transitional stratigraphic boundary between the lower Tistung Formation and the upper Chandragiri Limestone. It is primarily composed of slate, with minor sandstone and limestone, and is structurally deformed with several small-scale folds. An S-type fold identified 250 m north of Osho Tapoban in grey slate shows late-stage compressional deformation. Overall, the observed lithological assemblages and structural features reflect a multiphase tectonometamorphic history involving sedimentation, regional metamorphism, partial melting, and later deformation phases, shaping the current architecture of the Kathmandu Complex.

Based on the observed mineral assemblages in thin sections, along with field-based lithological and stratigraphic observations, a stratigraphic correlation has been proposed for the study area (see Table 2). In the stratigraphic correlation proposed by Stöcklin (1980) and Stöcklin and Bhattarai (1977), units such as the Chandragiri Limestone, Sopyang Formation, and Tistung Formation are assigned to the Phulchauki Group within the Lesser Himalayan sequence and the present study results are also align with those past studies. An unconformity separates the overlying higher-grade metamorphic rocks from the lower formations. Above this boundary, lithological units such as pegmatite, granite, augen gneiss, migmatite, banded gneiss, and calc-silicate gneiss are identified and are collectively attributed to the Markhu Formation. These are interpreted as part of the Higher Himalayan Sequence. Similarly, the Kulikhani Formation observed in the study area aligns with the unit described in earlier works and represents part of the metamorphosed sequence within the Phulchauki Group. This correlation reflects a consistent lithostratigraphic framework, confirming earlier models with refinements based on petrographic and structural evidence from the current fieldwork.

The lithological and petrographic investigations across the study area reveal a complex metamorphic history and diverse rock assemblages, reflecting multiple phases of deformation and recrystallization. Graphitic schists observed in the middle sections of the Kulikhani Formation are characterized by a high concentration of graphite and well-developed foliation defined by aligned mica and quartz. The presence of biotite and preferred mineral orientation points to regional metamorphism and deformation under moderate-grade conditions. Quartzites of the Kulikhani Formation show high quartz content with inequigranular textures and interlobate to amoeboid grain boundaries. Indicators such as foam-like textures, triple junctions, bulging, and sub-grain formation suggest the coexistence of dynamic and static recrystallization, implying episodes of both rapid deformation and slow cooling. Phyllites from the lower part of the Kulikhani Formation exhibit alternating bands of micaceous and quartz-rich layers. The fine-grained quartz and aligned mica and sericite form a distinct foliation. Features like grain boundary migration and preserved relict grains within quartz highlight dynamic recrystallization processes, consistent with higher-temperature deformation regimes. Garnet-bearing schists in the upper Kulikhani Formation include quartz, mica, and porphyroblastic garnets. Garnets show random internal inclusion patterns, indicating a pre-tectonic growth phase. Shear sense indicators like asymmetric garnet strain shadows confirm ductile deformation with top-to-the-south shearing. Ortho-gneiss and banded gneiss samples from the central gneissic zone are composed mainly of quartz, feldspar, and mica, with some exhibiting large feldspar porphyroclasts. Deformation features such as undulose extinction, foam-like textures, and mica fish suggest a high-grade metamorphic environment. Grain boundary migration and bulging are common, reflecting dynamic recrystallization during high-temperature conditions (approximately 500–700°C). Granitic gneisses display characteristic textures of high-temperature metamorphism, such as sutured and amoeboid quartz grains, large plagioclase crystals, and high-relief biotite. Evidence of recrystallization includes both grain boundary migration and bulging mechanisms, confirming intense deformation and thermal events. Calc-silicate rocks show mineral assemblages dominated by quartz, calcite, and feldspar. Sutured grain boundaries, calcite twinning, and lamellar structures indicate deformation under metamorphic conditions. These features are consistent with grain boundary migration during dynamic recrystallization, supporting interpretations of high-pressure–temperature regimes. Metasandstones in the southern section contain fine-grained quartz with folded and irregular boundaries, along with biotite, muscovite, and chlorite. Such textures indicate rapid recrystallization due to deformation. Irregular and folded grain contacts further support the occurrence of grain boundary migration and other recrystallization processes. Marble and dolomitic limestones from the Sopyang Formation consist primarily of calcite and dolomite, displaying characteristic twinning and 120° triple junctions. These features reflect grain boundary area reduction and crystal plasticity during recrystallization. The preservation of twinned structures suggests deformation under low- to medium-temperature metamorphic conditions. Overall, the petrographic evidence across the study area reveals a metamorphic evolution characterized by dynamic recrystallization, grain boundary migration, and mineralogical re-equilibration. These processes reflect tectonic activities associated with the Himalayan orogeny, where compressional stresses, temperature variations, and fluid movements played critical roles in the deformation and metamorphism of these rocks. The dominant recrystallization mechanisms identified are bulging (BLG), grain boundary migration (GBM), pinning, and grain boundary area reduction (GBAR). These processes occur in spatial patterns across the study area and are indicative of varying metamorphic conditions. In the northern section, microstructures such as bulging, pinning, window structures, and triple junctions suggest recrystallization at lower temperatures, typically in the range of 300-400°C (Passchier and Trouw, 2005). These features point to dynamic recrystallization under relatively low-grade metamorphic conditions. In contrast, the central region shows evidence of GBM and pinning, implying recrystallization under intermediate to high temperature conditions, approximately 500–700°C (Passchier and Trouw, 2005). This temperature range reflects a transition zone where rocks experienced more intense deformation and metamorphism. Near the thrust zone and within the gneissic units, features associated with GBAR are prevalent, often occurring after GBM. These microstructures, together with foam-like textures and triple junctions, indicate recrystallization at higher temperatures, around 700°C (Passchier and Trouw, 2005), and are consistent with conditions favoring static recrystallization. Overall, these observations suggest that rocks from the Lesser Himalayan Sequence were deformed and recrystallized under medium to high temperatures (300–700°C), primarily through dynamic recrystallization mechanisms. In contrast, rocks from the Higher Himalayan Sequence experienced higher temperature conditions (~700°C), with signatures of static recrystallization. This spatial variation in microstructural features reflects the tectonometamorphic evolution across the study area and highlights the differential thermal regimes associated with crustal-scale thrusting and deformation.

Table 2: Correlation of Lithological units from the Kathmandu Complex with present study area

Stöcklin (1980); and Stöcklin and Bhattarai (1977)	Present Study	Rock Unit
Chandragiri Limestone	Chandragiri Limestone	Phulchauki Group
Sopyang Formation	Sopyang Formation	
Tistung Formation	Tistung Formation	
----unconformity------		
Markhu Formation	Pegmatite, Granite, gneiss (augen gneiss, Migmatite, banded, calc-silicate gneiss)	Phulchauki Group
Kulekhani Formation	Kulikhani Formation	

CONCLUSIONS

The geological investigation of the study area reveals a distinct lithological and structural distribution dominated by the Kulikhani Formation (Bhimphedi Group) and several units of the Phulchauki Group, including the Tistung, Sopyang, and Chandragiri formations. The northern region is characterized by micaceous and graphitic schists, while the central region is dominated by various types of gneiss, including augen, banded, hornblende, calc-silicate, and migmatite gneiss, indicating high-grade metamorphism. Pegmatite intrusions, both tourmaline- and biotite-rich, are common and structurally concordant in places. The southern formations consist of phyllite, metasandstone, slate, and limestone, reflecting lower-grade metamorphism and sedimentary origins. The presence of structures like ptygmatic folds, foliation-parallel pegmatites, and small-scale folding within slates supports a complex deformation and metamorphic history, reflecting the tectonometamorphic evolution of the Kathmandu Complex.

Petrographic analysis of 14 representative rock samples from the study area reveals a diverse range of metamorphic and sedimentary lithologies, reflecting a complex tectonometamorphic history. Graphitic schist (R1) and phyllite (R3, R4) show well-developed foliation with abundant quartz, mica, and biotite, indicating moderate- to high-grade metamorphism. Quartzites (R2) and metasandstones (R13) show clear features of dynamic and static recrystallization such as grain boundary migration (GBM), bulging (BLG), and window structures, suggesting deformation under elevated temperatures. Gneissic samples (R6, R7, R8, R9, R10) show strong evidence of high-temperature metamorphism with foam-like textures, sutured grain boundaries, and large feldspar grains. Garnet-bearing schists (R3) and calcsilicate rocks (R11) further confirm metamorphic conditions ranging from medium to high grade. Calcite and dolomite-rich limestones (R13, R14) from the Sopyang Formation exhibit triple junctions, twinning, and recrystallization textures, typical of deformation under low- to medium-grade metamorphism. The widespread presence of dynamic recrystallization textures across rock types suggests intense tectonic activity and prolonged deformation across the study region.

ACKNOWLEDGEMENTS

The authors express their sincere gratitude to the Central Department of Geology, Tribhuvan University, for providing access to laboratory facilities essential for thin section preparation and petrographic analysis**.** Special thanks to Bhima Sharma for her valuable assistance during field studies and sample collection.

REFERENCES

Acharya, R., and Paudyal, K., 2015, Petrography of Low-Grade Metamorphic Rocks of the Lesser Himalaya from Malekhu Area, Central Nepal.

Arita, K., 1983, Origin of the inverted metamorphism of the Lower Himalayas, central Nepal. Tectonophysics, v. 95(1-2), pp. 43-60.

Auden, J., 1934, The geology of the Krol belt. Rec. Geol. Surv. India, v. 67(4), pp. 357-454.

Bordet, P., 1972, Some features of the geology of the Annapurna Range, Nepal Himalaya. Himalayan Geology, v. 2, pp 537-563.

Colchen, M., Le Fort, P., and Pêcher, A., 1986, Annapurna, Manaslu, Ganesh, Himal: notice de la carte géologique au 1/200,000 e: Editions du Centre national de la recherche scientifique.

Coward, M., and Butler, R., 1985, Thrust tectonics and the deep structure of the Pakistan Himalaya. Geology, v. 13(6) pp. 417-420.

Dhital, M. R., Sunuwar, S. C., and Shrestha, R., 2002, Geology and structure of the Sundarijal–Melamchi area, central Nepal. Paper presented at the Third Nepal Geological Congress.

Dhital, M. R., Thapa, P. B., Ando, H., 2002, Geology of the inner Lesser Himalaya between Kusma and Syangja in western Nepal. Bulletin of Department of Geology, Tribhuvan University, v. 9 (Special Issue), pp. 1-60.

Dewey, J. F., and Bird, J. M., 1970, Mountain belts and the new global tectonics. Journal of Geophysical Research, v. 75(14), pp. 2625-2647.

Hagen, T., 1969, Report on the geological survey of Nepal. Denkschr. Schweiz. Naturf. Ges., v. 81, pp. 185.

Hashimoto, S., and Ohta, Y., 1973, Geology of the Nepal Himalayas.

Heim, A., and Gansser, A., 1975, Central Himalaya: Geological observations of the Swiss expedition. Hindustan Publishing Corporation (India), v. 73

Johnson, M., Oliver, G. J. H., Parrish, R., and Johnson, S., 2001, Synthrusting metamorphism, cooling, and erosion of the Himalayan Kathmandu Complex, Nepal. Tectonics, v. 20(3), pp. 394-415.

Le Fort, P, 1975, Les formations cristallophyliennes de la “Dalle du Tibet” en Marsyandi, Recherches geologiques dans l’Himalaya du Nepal region du Nyi-Shang, pp. 21-47.

Le Fort, P., 1986, Metamorphism and magmatism during the Himalayan collision. In: Coward, M.P., Ries, A. (Eds.), Collision Tectonics, Geological Society Special Publication, v. 19 pp. 159 -172

Le Fort, P., 1996, Evolution of the Himalaya. In: Yin A, Harrison TM (eds) The tectonics of Asia, Cambridge University Press, New York, pp. 95–106.

Passchier, C. W., and Trouw, R. A. J., 2005, MicroTectonics. Springer-Verlag 2nd edition, Berlin, pp. 289.

Passchier, C. W., and Trouw, R. A. J., 2015, Atlas of Mylonites and related structures. Springer-Verlag, Berlin, pp. 305.

Paudel, L. P., and Arita, K., 2000, Tectonic and polymetamorphic History of the Lesser Himalaya in the central Nepal. Journal of Asian Earth Sciences, pp. 10-24.

Paudel, L. P., and Arita, K., 2006, Thermal evolution of the Lesser Himalaya, central Nepal: Insights from K-white micas compositional variation. Gondwana Research, v. 9, pp. 409-425

Paudel, L. P., 2008, Petrographic records of two metamorphic events in the Lesser Himalayan metabasites, Modi Khola section, central Nepal. Bulletin of the Department of Geology, Tribhuvan University, Nepal, v. 11, pp. 5-12.

Paudyal, K. R., and Paudel, L. P., 2013, Geological study and root zone interpretation of the Kahun Klippe, Tanahu, and central Nepal. Himalayan Geology, v. 34(2), pp. 93-106.

Paudyal, K. R., 2014, Geological and Petrological Evolution of the Lesser Himalaya between Mugling and Damauli, central Nepal.

PhD thesis, Tribhuvan University, Central of the Department of Geology, pp. 217

Pêcher, A., 1989, The metamorphism in the central Himalaya. Journal of Metamorphic Geology, v. 7, pp. 31-41.

Rai, S., 1998, Etude structurale, metamorphique, geochimique et radiochronologique des nappes deKatmandou et du Gosainkund, Himalaya du Nepal central. Ph. D. thesis, Univ. Joseph Fourier, Grenoble, France.

Sharma, C., 1990, Geology of western Nepal Chapter 14, Geology of Nepal and Adjacent Countries,164 p.

Sapkota, J., 2011, Structure, metamorphism and tectonics of the central Nepal Himalayas. PhD thesis submitted to School of the Earth and Environmental Sciences, James Cook University, Australia, v. I, p. 109, http://eprints.jcu.edu.au/26380.

Stöcklin, J., 1980, Geology of Nepal and its regional frame: Thirty-third William Smith Lecture. Journal of the Geological Society, v. 137(1), pp. 1-34.

Stöcklin, J., and Bhattarai, K. D., 1977, Geology of Kathmandu Area and Central Mahabharat Range, Nepal Himalaya. Report of Department of Mines and Geology/UNDP (unpublished), p. 86.

Thapaliya, S., Silwal, B., L. P., 2011, Geology, lithostratigraphy and petrography of the Kakani- Trishuli area, central Nepal. Bulletin of Department of Geology, Tribhuvan University, Kathmandu, Nepal, Masters thesis.

Thapaliya, S., and Paudel, L. P., 2011, Inverted metamorphic zonation in the hanging and foot walls of the Mhabharat Thrust, Kathmandu-Trishuli area, central Nepal. Bulletin of Department of Geology, Tribhuvan University, Kathmandu, Nepal, v. 14, pp. 51-58.

Upreti, B. N., 1999, An overview of the stratigraphy and tectonics of the Nepal Himalaya. Journal of Asian Earth sciences, v. 17, pp. 577-606.

Upreti, B. N., Le Fort, P., 1999, Lesser Himalayan crystalline nappes of Nepal: problem of their origin. In: Macfarlane, A., Quade, J., Sorkhabi, R. (Eds.), Geological Society of America Special paper, v. 328, pp. 225-238.